

1 **Messinian palaeoproductivity changes in the northeastern Atlantic and its relation**
2 **to the closure of the Atlantic-Mediterranean gateway**

3
4 JOSÉ N. PÉREZ-ASENSIO^{1,*}, JULIO AGUIRRE¹, GERHARD SCHMIEDL² &
5 JORGE CIVIS³
6

7 *¹Departamento de Estratigrafía y Paleontología, Facultad de Ciencias, Avenida*
8 *Fuentenueva s.n., Universidad de Granada, 18002 Granada, Spain.*

9 *²Department of Geosciences, University of Hamburg, 20146 Hamburg, Germany.*

10 *³Departamento de Geología, Universidad de Salamanca, 37008 Salamanca, Spain.*

11 **Corresponding author (e-mail: jnoel@ugr.es)*
12

13 Number of words of text: 9313

14 References: 96

15 Tables: 1

16 Figures: 6
17

18 Abbreviated title: Messinian productivity in NE Atlantic
19

20 **Abstract**

21 The stable isotope composition of planktic and benthic foraminifera and
22 distribution of selected benthic foraminiferal species from a Messinian record of the
23 lower Guadalquivir Basin, northeastern Atlantic Ocean, show that regional productivity
24 changes were linked to glacioeustatic fluctuations. Glacial periods were characterized
25 by poorly ventilated bottom waters as a result of weak Atlantic meridional overturning

26 circulation (AMOC), and phases of high productivity related to intensified upwelling. In
27 contrast, well-ventilated bottom waters due to strong AMOC, and presence of degraded
28 organic matter in the upper slope and high input of degraded terrestrial organic matter
29 derived from riverine discharge in the outer shelf were recorded during interglacial
30 periods. Before the closure of the adjacent Guadalhorce Corridor at 6.18 Ma, the last
31 active Betic Atlantic-Mediterranean gateway, the study area was alternatively
32 influenced by the well-ventilated Mediterranean Outflow Water (MOW) and the poorly
33 ventilated Atlantic Upwelled Water (AUW). After the closure of the corridor, the
34 cessation of the MOW, which reduced the AMOC and promoted glacial conditions in
35 the northern hemisphere, resulted in the establishment of local upwelling cells.

36

37

38

39 Continental shelves and slopes play a fundamental role in the biogeochemical
40 cycling of carbon and nitrogen with equal importance than deep sea (Walsh 1991).
41 These areas present high-productivity ecosystems due to the supply of nutrients and
42 organic matter from both continental and marine sources. At present-day, regions under
43 upwelling influence represent areas with the highest primary productivity in the world's
44 ocean as evidenced by the massive populations of fishes, seabirds and marine mammals
45 supported by nutrients derived from upwelling (Bakun *et al.* 2010). In the present
46 Atlantic Ocean, the main upwelling areas are located in its eastern parts mainly along
47 the West African coast and the Iberian Peninsula because wind systems favoured
48 upwelling in the eastern coast of the Atlantic Ocean (Schmiedl *et al.* 1997; Martinez *et*
49 *al.* 1999; Bakun *et al.* 2010). Intensity and extent of upwelling currents are controlled
50 by Ekman pumping on the northern hemisphere, which is the vertical spiral movement

51 of bottom waters induced by strong northeasterly trade winds system and Coriolis force
52 (Tomczak & Godfrey 1994; Lebreiro *et al.* 1997).

53 The intensity of the upwelling currents has changed with glacial to interglacial
54 climate oscillations, eustatic sea-level fluctuations, and meridional temperature
55 gradients with higher upwelling intensity during glacial periods due to strong wind
56 stress (Lebreiro *et al.* 1997; Martinez *et al.* 1999; Salgueiro *et al.* 2010).
57 Palaeoproductivity proxies, including benthic foraminifera, diatoms, radiolarians, fish
58 debris, phosphorite grains, and stable C isotopes, show low C stable isotopic values and
59 high abundance of high-productivity organisms which is consistent with more intense
60 upwelling during glacial periods when upwelling-favourable trade winds were
61 intensified (Diester-Haass & Schrader 1979; Abrantes 1991, 2000; Martinez *et al.* 1999;
62 Eberwein & Mackensen, 2008). Furthermore, global palaeoceanographical circulation
63 patterns in the northern Atlantic also influenced productivity related to upwelling in the
64 region. It is very well established that the Mediterranean Outflow Water (MOW)
65 promote the North Atlantic deep water formation because supplies dense and saline
66 waters to the North Atlantic and therefore contributes to the Atlantic meridional
67 overturning circulation (AMOC) increasing the North Atlantic density gradient (Bigg &
68 Wadley, 2001; Bigg *et al.*, 2003; Rogerson *et al.* 2012). During Heinrich Events, a large
69 flux of freshwater was released in the North Atlantic decreasing density which led to the
70 collapse of the AMOC (McManus *et al.* 2004; Rogerson *et al.* 2010). Then, at the
71 earlier part of interglacial periods, the intensification and shoaling of the dense MOW
72 plume promoted the abrupt resumption of the AMOC (Rogerson *et al.* 2006, 2012).
73 Furthermore, a reduction or interruption of the Mediterranean Outflow Water would
74 result in a decrease or interruption of the North Atlantic deep water formation
75 (Rahmstorf 1998) and, consequently, would reduce the Atlantic meridional overturning

76 circulation declining the poleward heat transport in the Atlantic which would cause
77 cooling and ice sheet growth in the northern hemisphere (Zahn *et al.* 1997; Clark *et al.*
78 2002; McManus *et al.* 2004). This glaciation would lead to high-productivity conditions
79 due to stronger winds that induce Ekman pumping stimulating upwellings in the NE
80 Atlantic (Lebreiro *et al.* 1997; Zahn *et al.* 1997; Clark *et al.* 2002; Salgueiro *et al.*
81 2010).

82 Another source of organic matter in marine settings is terrestrial input via river
83 run-off close to the coast (McKee *et al.* 2004). High supply of terrestrial organic matter
84 can provide an important food resource for marine benthic ecosystems but its
85 degradation may also result in oxygen depletion of the bottom and pore waters (van der
86 Zwaan & Jorissen 1991; Jorissen *et al.* 1992; Donnici & Serandrei-Barbero 2002).
87 Shallow-water areas close to river mouths are excellent examples of high productivity
88 related to fresh water discharges. Under periods of increased river run-off, sediments
89 enriched in organic matter are discharged into the Atlantic Ocean by Iberian rivers such
90 as the Tagus and the Guadalquivir (Cabeçadas & Brogueira 1997; Lebreiro *et al.* 2006;
91 Villanueva-Guimerans & Canudo, 2008; Rodrigues *et al.* 2009). These periods of
92 intense riverine discharge are more frequent during warm periods due to increased
93 rainfall (Frei *et al.* 1998).

94 Palaeoproductivity in the northeastern Atlantic during the Pliocene, Pleistocene
95 and Holocene has been extensively studied (Lebreiro *et al.* 1997; Martinez *et al.* 1999;
96 van der Laan *et al.* 2006, Eberwein & Mackensen 2008; Naafs *et al.* 2010; Salgueiro *et*
97 *al.* 2010; Zariess & Mackensen 2010). According to these studies, intensification of the
98 African monsoon and the upwelling-favorable wind systems due to changes in global
99 climate controls the intensity and seasonality of primary productivity. In contrast,
100 information about productivity in the northeastern Atlantic during the Messinian is

101 scarce (van der Laan *et al.* 2006, 2012). These authors stated that riverine discharge in
102 the Atlantic off NW Morocco was higher during warm and wet interglacial periods.
103 These periods occurred during precession minima when summer insolation is maxima
104 and were related to enhanced winter rainfall linked to the Atlantic system (van der Laan
105 *et al.* 2012).

106 In terms of Messinian North Atlantic circulation, the cessation of the MOW at
107 6.18 Ma due to the closure of the Betic gateways produced the interruption of the North
108 Atlantic deep water and the intensification of the AMOC leading to a cooling in the
109 northern hemisphere (Pérez-Asensio *et al.* 2012a). Coincidentally, small or middle-scale
110 glaciations with small ice sheets development around the Iceland-Norwegian Sea took
111 place about 7-6 Ma (Fronval & Jansen 1996; Thiede *et al.* 1998). This is also indicated
112 by glacial records from Alaska, Baffin Bay, Iceland, and off SE Greenland (Fronval &
113 Jansen 1996). This cooling would have reduced surface water temperatures in the North
114 Atlantic enhancing trade winds that favoured high productivity related to upwelling
115 currents (Hughen *et al.* 1996; Clark *et al.* 2002). In fact, modelling studies suggest
116 intense northwesterly winds during the Messinian (Murphy *et al.* 2009). However, so
117 far, there is no detailed study focusing on the relationship of productivity changes in the
118 northeastern Atlantic with global climate and oceanography to prove this hypothesis.

119 In this study, foraminiferal stable oxygen and carbon isotope records and the
120 distribution of selected benthic foraminiferal species in the Montemayor-1 core (SW
121 Spain) have been analysed (Fig. 1). This core is located in the Guadalquivir Basin, an
122 open marine enbayment that constituted the Atlantic side of the Guadalhorce Corridor,
123 the last Betic Atlantic-Mediterranean gateway to be closed at 6.18 Ma (Martín *et al.*
124 2001, 2009; Pérez-Asensio *et al.* 2012a) (Fig. 1). According to benthic foraminiferal
125 assemblages, the Messinian record of the Montemayor-1 core represents a shallowing-

126 upward sequence including, from bottom to top, middle and upper-slope, shelf-edge and
127 outer-shelf deposits (Pérez-Asensio et al., 2012b) (Fig. 2). Furthermore, benthic
128 foraminifera indicate presence of upwelling currents in the upper slope and outer shelf
129 (Pérez-Asensio et al., 2012b) (Fig. 2). Middle-slope and part of the upper-slope
130 sediments were deposited under the influence of the MOW before the closure of the
131 Guadalhorce seaway at 6.18 Ma (Pérez-Asensio *et al.* 2012a). After 6.18 Ma, part of the
132 upper slope setting, the shelf edge and outer shelf were not affected by the MOW.
133 Palaeoceanographical changes produced by the MOW interruption affected the global
134 oceanography and climate leading to a cooling in the northern hemisphere (Pérez-
135 Asensio *et al.* 2012a). Therefore, the location of this core is exceptional: (1) to
136 investigate the productivity changes and organic carbon cycling in the eastern North
137 Atlantic during the Messinian; (2) to assess the effect of the cessation of the MOW at
138 6.18 Ma on the Messinian palaeoproductivity; and (3) to decipher the relationship
139 between productivity and global oceanography and climate.

140

141 **Geographical and geological setting**

142

143 The study area is located in the northwestern margin of the lower Guadalquivir
144 Basin (SW Spain) (Fig. 1). This basin is an ENE-WSW elongated Atlantic foreland
145 basin which is bounded to the N by the Iberian Massif, to the S by the Betic Cordillera,
146 and to the W by the Atlantic Ocean (Sanz de Galdeano & Vera 1992; Vera 2000; Braga
147 *et al.* 2002). The sedimentary filling of the basin consists of marine deposits ranging
148 from the early Tortonian to the late Pliocene (Aguirre 1992, 1995; Aguirre *et al.* 1995;
149 Ríaza & Martínez del Olmo 1996; Sierro *et al.* 1996; Braga *et al.* 2002; González-
150 Delgado *et al.* 2004; Martín *et al.* 2009).

151 The Guadalquivir Basin acted as a corridor, the so-called North-Betic Strait,
152 connecting the Atlantic and the Mediterranean during the earliest Tortonian (Aguirre *et*
153 *al.* 2007; Martín *et al.* 2009; Braga *et al.* 2010). Other Betic seaways that connected the
154 Atlantic and the Mediterranean through the Guadalquivir Basin after the closure of the
155 North Betic Strait during the early Tortonian, were gradually closed during the late
156 Miocene (Esteban *et al.* 1996; Martín *et al.* 2001; Braga *et al.* 2003; Betzler *et al.* 2006;
157 Martín *et al.* 2009). The Guadalhorce Corridor was the last active Betic corridor and
158 was closed in the early Messinian (Martín *et al.* 2001; Pérez-Asensio *et al.* 2012a).
159 After its closure, the only Atlantic-Mediterranean connections were established through
160 the Rifian Corridors, northern Morocco (Esteban *et al.* 1996).

161 In the study area, Neogene deposits that filled the lower Guadalquivir Basin
162 have been divided into four lithostratigraphic units formally described as formations.
163 From bottom to top: (1) carbonate-siliciclastic mixed deposits of the Niebla Formation
164 (Civis *et al.* 1987; Baceta & Pendón 1999); (2) greenish-bluish clays of the Arcillas de
165 Gibraleón Formation (Civis *et al.* 1987); (3) fossiliferous sands and silts of the Arenas
166 de Huelva Formation (Civis *et al.* 1987); and (4) sands of the Arenas de Bonares
167 Formation (Mayoral & Pendón 1987).

168

169 **Materials and methods**

170

171 The studied material is the 260 m long continuous Montemayor-1 core, which is
172 located close to Huelva (SW Spain) (Fig. 1). This core includes sediments from the four
173 aforementioned formations (see a summary in Pérez-Asensio *et al.* 2012b) (Fig. 3). The
174 age model of the core is based on magnetobiostratigraphy and glacial stages TG 22 and
175 12, and interglacial stage TG 7 obtained from O stable isotope data (Larrasoña *et al.*

176 2008; Pérez-Asensio *et al.* 2012a, Jiménez-Moreno *et al.* 2013) (Fig. 3). In this work,
177 an interval of 140 m, from 240 to 100 m, which ranges from 6.67 to 5.38 Ma
178 (Messinian), has been studied. This interval includes marine sediments from the Arcillas
179 de Gibrleón Formation (Fig. 3).

180 For faunal analysis, a total of 255 samples were collected with a sampling
181 interval of 0.5 m. As shown in the age model (Fig. 3), there is a significant change of
182 sedimentation rate along the core. As a consequence, the average temporal resolution of
183 samples is 28.68 kyr from 240 m to 218.5 m (base of chron C3r) and 2.75 kyr from
184 218.5 m to 100 m. Samples were wet sieved over a 63 µm mesh and dried out in an
185 oven at 40 °C. Using a microsplitter samples were divided into sub-samples containing
186 at least 300 benthic foraminifera. The sub-samples were dry sieved over a 125 µm
187 mesh, and benthic foraminifera were identified and counted. Benthic foraminiferal
188 counts were transformed into relative abundances. In order to assess changes in flux
189 rates, provenance and degradation state of organic matter we used the relative
190 abundances of high-productivity target taxa including *Uvigerina peregrina* s.l. (*U.*
191 *peregrina* + *U. pygmaea*), *Bulimina subulata*, *Brizalina spathulata*, and *Bulimina*
192 *aculeata* (Donnici & Serandrei-Barbero 2002; Schmiedl & Leuschner 2005; Murray
193 2006; Diz & Francés 2008; Duchemin *et al.* 2008; Schmiedl *et al.* 2010). In addition,
194 changes in the oxygen content were analysed using the palaeo-oxygenation index of
195 Schmiedl *et al.* (2003): $[\text{HO}/(\text{HO}+\text{LO})+\text{Div}] \times 0.5$. In this formula, HO is the relative
196 abundance of high oxygen indicators (epifaunal taxa), LO is the relative abundance of
197 low oxygen indicators (deep infaunal taxa), and Div is normalized benthic foraminiferal
198 diversity using the Shannon index (H) calculated with the software PAST (Hammer *et*
199 *al.* 2001).

200 For stable oxygen and carbon isotope analyses, a total of 160 samples were
201 analysed. The sampling interval is 0.5 m from 240 to 170 m, and 2.5 m from 170 to 100
202 m. Around 10 tests of *Cibicidoides pachydermus* and 20 tests of *Globigerina bulloides*
203 have been picked from the size fraction >125 μm . Prior to the analyses, presence of
204 diagenetic alterations was discarded checking dissolution and/or recrystallization of
205 shells under the SEM. Foraminifera were cleaned with ultrasonic bath and washed with
206 deionized water. Samples were analysed at the Leibniz-Laboratory for Radiometric
207 Dating and Isotope Research, Kiel, Germany. The stable isotope analyses were
208 performed on a Finnigan MAT 251 mass spectrometer connected to a Kiel I (prototype)
209 preparation device for carbonates. Results are presented in δ -notation (‰), and
210 standardised to the Vienna Pee Dee belemnite (VPDB) scale. This scale is defined by a
211 certain value of the National Bureau of Standards (NBS) carbonate standard NBS-19.
212 The international and lab-internal standard material indicate that the analytical
213 reproducibility is $< \pm 0.05$ ‰ for $\delta^{13}\text{C}$, and $< \pm 0.07$ ‰ for $\delta^{18}\text{O}$.

214 Additionally, Pearson correlation coefficients were calculated to assess the
215 statistical correlation between O and C stable isotopes, relative abundance of target taxa
216 and planktonic/benthonic (P/B) ratio, this last metric following Pérez-Asensio *et al.*
217 (2012b) (Table 1). Only coefficients with a p -value < 0.01 or < 0.05 were considered
218 significant.

219

220 **Results**

221

222 *High-productivity target taxa and palaeo-oxygenation index*

223

224 The relative abundance of *Uvigerina peregrina* s.l. shows relatively high values
225 from 6.67 to 5.87 Ma (Fig. 4). In this interval, it presents two significant minima at
226 around 6.44 and 6.24 Ma, and two maxima at 6.67 and 6.35 Ma. Then, it gradually
227 increases from 6.18 to 5.87 Ma (Fig. 4). This species sharply diminishes at 5.87 Ma
228 (Fig. 4). In the interval from 5.87 to 5.38 Ma, it has low average values around 10%
229 (Fig. 4). *Bulimina subulata* is more abundant from 6.67 to 5.85 Ma (Fig. 4). In the
230 interval from 5.87 to 5.38 Ma, *B. subulata* experiences a gradual decrease. In contrast,
231 *Brizalina spathulata* and *Bulimina aculeata* are more abundant between 5.87 and 5.38
232 Ma (Fig. 4). In this interval, both species progressively replace *B. subulata*.

233 The palaeo-oxygenation index shows relatively high values (>0.8) along the
234 studied interval (Fig. 5). Furthermore, some oxygen depletions are recorded at 6.00,
235 5.99, 5.96, 5.91, and 5.87 Ma. In the interval from 5.87 to 5.38 Ma, there are oxygen
236 depletions higher than before 5.87 Ma.

237

238 *Stable isotope data*

239

240 The benthic oxygen isotope record measured in *Cibicidoides pachydermus* has
241 stable average values of +1‰ before 6.35 Ma, followed by a decrease of 1.9‰ until a
242 minimum of -0.9‰, which is reached at 6.18 Ma (Figs 4 and 5). In the interval from
243 6.18 to 5.79 Ma, it gradually increases toward heavier values with a total increase of
244 0.3‰. Finally, $\delta^{18}\text{O}$ values decrease 1.20‰ from 5.79 to 5.72 Ma and remain at
245 relatively low values ($\sim +0.4\text{‰}$) from 5.72 to 5.38 Ma (Figs 4 and 5). The planktic
246 (*Globigerina bulloides*) oxygen isotope record shows a fluctuating trend with average
247 values lower than 0‰ before 6.18 Ma (Figs 4 and 5). In the interval from 6.18 to 5.79
248 Ma, the values progressively increase with a total increase of 1.20‰ (Figs 4 and 5).

249 After 5.79 Ma, the planktic oxygen isotope record exhibits two drops at 5.75 Ma and
250 5.52 Ma; 0.8‰ and 1‰ respectively. The planktic and benthic $\delta^{18}\text{O}$ curves exhibit
251 similar trends, especially from 6.18 Ma onwards, as it is also indicated by the positive
252 correlation (Table 1).

253 The benthic carbon isotope record presents a fluctuating trend with average
254 values of +0.4‰ before 6.18 Ma (Figs 4 and 5). Then, $\delta^{13}\text{C}$ decreases 0.8‰ from 6.18
255 to 5.9 Ma and it remains at values around +0.4‰ from 5.9 to 5.67 Ma. Finally, it
256 gradually decreases 0.7‰ from 5.67 to 5.38 Ma. The planktic carbon isotopic values
257 show fluctuations around values of -0.8‰ before 6.18 Ma (Figs 4 and 5). Subsequently,
258 $\delta^{13}\text{C}$ diminishes 1.3‰ reaching its lowest values from 6.05 to 5.85 Ma. At 5.85 Ma, the
259 planktic carbon isotope record abruptly rises from -1‰ to 0‰ and it remains with high
260 average values of 0‰ until 5.77 Ma. Then, it sharply decreases up to -1‰ and it
261 increases until values of 0‰ at 5.67 Ma. Finally, it gradually diminishes 1.4 ‰ from
262 5.67 to 5.38 Ma.

263 Comparing the stable isotope record with the high-productivity target taxa, high
264 values of the benthic and planktic $\delta^{18}\text{O}$ coincide with low benthic $\delta^{13}\text{C}$ values, and high
265 abundance of *Uvigerina peregrina* s.l. and low abundance of *Bulimina subulata* (Fig.
266 4). In the interval between 5.67 and 5.38 Ma, low benthic and planktic $\delta^{18}\text{O}$ values
267 concur with low benthic and planktic $\delta^{13}\text{C}$ values and high percentages of *Brizalina*
268 *spathulata* and *Bulimina aculeata*.

269

270 **Discussion**

271

272 *Palaeoproductivity changes and organic carbon cycling in the northeastern Atlantic*
273 *during the Messinian*

274

275 Our results suggest that palaeoproductivity changes and organic carbon cycling
276 in the northeastern Atlantic depended on the global glacioeustatic fluctuations that, in
277 turn, affected the distribution of the high-productivity benthic foraminiferal species. In
278 addition to these global palaeoceanographical processes, benthic foraminiferal and
279 palynomorph (pollen and dinocysts) assemblages from the Montemayor-1 core suggest
280 a shallowing upwards trend from upper slope to outer platform settings (Pérez-Asensio
281 *et al.* 2012*b*; Jiménez-Moreno *et al.* 2013). Thus, effects of the local
282 palaeoenvironmental evolution of this region of the lower Guadalquivir Basin were
283 superimposed to the global glacioeustatic variations.

284 In the upper slope deposits of the study core (from 246.5 to 194 m core depth),
285 glacial periods characterized by high planktic and benthic O isotopic values coincide
286 with low benthic $\delta^{13}\text{C}$ values (Fig. 4). This is supported by marginal negative
287 correlation between planktic O and benthic C isotopic values (Table 1). Furthermore,
288 fluctuations in the benthic $\delta^{13}\text{C}$ are around $\pm 0.5\%$ (Figs 4 and 5). The glacial decrease
289 in the $\delta^{13}\text{C}$ was between 0.46 and 0.32‰ during glacial-to-interglacial fluctuations in
290 the global C budget in the Quaternary (Piotrowski *et al.* 2005). Messinian changes in
291 global C budget, however, might have been smaller than during the Quaternary due to
292 weaker glacial-interglacial contrasts and related vegetation changes, as well as shelf
293 exposures. Therefore, other factors together with changes in the global C budget should
294 have contributed to the observed benthic $\delta^{13}\text{C}$ signature, such as influence of nutrient-
295 rich waters and/or residence time of water masses. In general, benthic $\delta^{13}\text{C}$ values are
296 low in areas of high primary productivity (Mackensen 2008). At the present day and

297 during the Holocene, low benthic $\delta^{13}\text{C}$ signatures are indicative of high productivity
298 related to upwelling currents in NW Africa (Morocco) (Eberwein & Mackensen 2006,
299 2008). During regressions, input of refractory organic matter with isotopically light
300 carbon from the exposed continental shelf also produces low benthic $\delta^{13}\text{C}$ values as
301 recorded in late Miocene sediments from the tropical Indian Ocean and Mediterranean
302 Sea (Vincent *et al.* 1980; Loutit & Keigwin 1982; Kouwenhoven *et al.* 1999) Thus, the
303 low $\delta^{13}\text{C}$ values in the upper slope deposits were related either to the influence of
304 nutrient-rich intermediate waters, like upwelling currents from a distant source area, or
305 to the remineralisation of refractory organic matter reworked from exposed continental
306 shelf sediments during sea-level lowstands.

307 Upper slope deposits are characterized by the abundance of the *Uvigerina*
308 *peregrina* s.l. (Pérez-Asensio *et al.* 2012b) (Fig. 4). This shallow-infaunal species is
309 characteristic of mesotrophic conditions (e.g. Schmiedl *et al.* 2000; Phipps *et al.* 2012)
310 and prefers fresh marine organic matter as food source (Fontanier *et al.* 2003; Koho *et*
311 *al.* 2008; Schmiedl *et al.* 2010). In the study area, elevated productivity is likely
312 attributed to upwelling currents as explained above (Fig. 2), which is also consistent
313 with the observed negative correlation between *U. peregrina* s.l. and benthic C isotopic
314 values (Table 1). This, in turn, points to the influence of distant intermediate waters that
315 were upwelling currents from the Atlantic Ocean. Furthermore, these high-productivity
316 conditions occurred during glacial periods as indicated above and supported by
317 observations from equivalent modern environmental settings (Schmiedl *et al.* 1997;
318 Mendes *et al.* 2004; Martins *et al.* 2006; Mojtahid *et al.* 2006). The marginal positive
319 correlation between *U. peregrina* s.l. and benthic O isotopic values also suggests high
320 productivity during glacial periods (Table 1). The driving mechanism for enhanced
321 upwelling in the lower Guadalquivir Basin might be stronger winds promoting Ekman

322 pumping during glacial periods as occurred in the Quaternary (Lebreiro *et al.* 1997;
323 Schmiedl & Mackensen 1997; Poli *et al.* 2010; Salgueiro *et al.* 2010). Wind intensity
324 and direction have been analysed in the modelling study of Murphy *et al.* (2009). This
325 study includes three simulations considering 1) a desiccated Mediterranean Sea with a
326 sea-level reduced 750 m, 2) a desiccated Mediterranean Sea with a sea-level reduced
327 1500 m, and 3) a not desiccated Mediterranean Sea with a sea-level reduced 1500 m.
328 Both simulations with a reduction of 1500 m in sea-level shows intense northwesterly
329 winds during the Messinian which might enhance upwelling as occur at the present day
330 when northerly winds promote upwelling (Lebreiro *et al.* 1997).

331 The effect of upwelling currents is also confirmed by the negative correlation
332 between planktic C isotopes and *U. peregrina* s. l. (Table 1). The low planktic $\delta^{13}\text{C}$
333 values from the Montemayor-1 core are due to the fact that they have been measured in
334 *Globigerina bulloides*, which inhabits waters from surface to intermediate depths (20-
335 300 m) (Pujol & Vergnaud-Grazzini 1995). Therefore, this species is likely reflecting
336 the isotopic signature of nutrient-rich ^{13}C -depleted upwelling intermediate waters
337 masses. Furthermore, the $\delta^{13}\text{C}$ of *G. bulloides* decreases during upwelling events
338 because of the fractionation of carbon isotopes due most likely to vital effects (Lebreiro
339 *et al.* 1997; Naidu & Niitsuma 2004). During strong upwelling faster calcification rates
340 due to high-nutrient availability requires higher respiration, which involves more
341 respired CO_2 enriched in ^{12}C (Naidu & Niitsuma 2004). Additionally, release of ^{12}C
342 during decomposition of organic matter in the lower part of the photic layer could
343 contribute to the low $\delta^{13}\text{C}$ of *G. bulloides*. These combined effects would explain the
344 very low planktic $\delta^{13}\text{C}$ signatures along the Montemayor-1 core.

345 According with the benthic foraminiferal assemblages in the upper slope
346 deposits (Pérez-Asensio *et al.* 2012b), peaks of relative abundance of *U. peregrina* s.l.

347 during glacial periods alternate with high percentages of *Bulimina subulata* (Fig. 4).
348 *Bulimina subulata*, like other species of the genus, feeds from more degraded organic
349 matter (Schmiedl *et al.* 2000; Diz & Francés 2008) than *Uvigerina peregrina* s.l., which
350 feeds from fresh and labile organic matter (Fontanier *et al.* 2003; Koho *et al.* 2008;
351 Schmiedl *et al.* 2010). This difference in trophic behavior might account for the low
352 abundances of *B. subulata* during glacial periods when fresh organic matter was
353 available on the sea-floor. In contrast, *B. subulata* was abundant during interglacial
354 periods suggesting presence of more degraded marine organic matter.

355 *U. peregrina* s.l. and *B. subulata* abundances decrease in a different way after
356 5.87 Ma (Fig. 4). At this age, *Uvigerina peregrina* s.l. virtually disappears while *B.*
357 *subulata* diminishes gradually. On the upper slope, *U. peregrina* s.l. is replaced by
358 epifaunal taxa, mainly *P. ariminensis*, inhabiting an oligotrophic shelf edge setting
359 (Pérez-Asensio *et al.* 2012b). This sharp decrease of *U. peregrina* s.l. was due to the
360 absence of fresh organic matter in the required quantity because upwelling currents did
361 not reach the shelf edge (Fig. 2). In contrast with low planktic $\delta^{13}\text{C}$ values during high
362 productivity conditions produced by upwelling as recorded in Holocene sediments from
363 the NE Atlantic Ocean off Portugal (Lebreiro *et al.* 1997), relatively high planktic $\delta^{13}\text{C}$
364 values suggests presence of nutrient-depleted intermediate water masses on the shelf
365 edge (Fig. 4). Such an oligotrophic setting during glacial conditions may have been
366 caused by the establishment of a contour current flowing along the platform margin
367 preventing upwelling intermediate waters from reaching the shelf edge (Fig. 2). In
368 contrast, *B. subulata* diminishes more gradually because there was no fresh organic
369 matter on the shelf edge, but more degraded organic matter was still present at the sea
370 floor, and *B. subulata* was able to feed from this degraded organic matter.

371 At 5.77 Ma, *Planulina ariminensis* disappears pointing to the transition from the
372 shelf edge to the outer shelf (Pérez-Asensio *et al.* 2012b) (Fig. 2). This event was
373 concomitant with a significant sea-level drop close to the glacial stage TG 20 (5.75 Ma)
374 (Pérez-Asensio *et al.* 2012a, 2012b; Jiménez-Moreno *et al.* 2013). From 5.77 to 5.67
375 Ma, the planktic $\delta^{13}\text{C}$ experienced a significant increase of 1‰ (Fig. 4) pointing to a
376 decrease in the productivity most likely related to less influence of upwelling currents
377 during interglacial conditions as it is shown by the decrease of 0.9‰ in benthic $\delta^{18}\text{O}$
378 (Fig. 4). After 5.67 Ma, the outer-shelf setting was characterized by high abundance of
379 *Brizalina spathulata* and *Bulimina aculeata* (Pérez-Asensio *et al.* 2012b) (Fig. 4). It is
380 well established that *B. spathulata* can thrive with continental degraded organic matter
381 derived from river run-off (Donnici & Serandrei-Barbero 2002; Duchemin *et al.* 2008;
382 Schmiedl *et al.* 2010). Concomitantly, the upwelling-related *U. peregrina* s.l. shows
383 high relative abundances during glacial periods, whereas *B. spathulata* has relatively
384 low values. This is supported by a negative correlation between both species (Table 1).
385 Hence, *B. spathulata* does not seem to have been controlled by the influence of fresh
386 organic matter derived from upwelling currents, as previously interpreted (Pérez-
387 Asensio *et al.* 2012b).

388 *B. aculeata* is able to feed from both fresh and degraded organic matter
389 (Schmiedl & Leuschner 2005). It has been also found in low-oxygen environments with
390 supply of continental degraded organic matter under river run-off influence (Schmiedl
391 *et al.* 2000, Pérez-Asensio & Aguirre 2010). In the study site, it shows the highest
392 percentages coinciding with high values of *B. spathulata* during interglacial periods
393 (Fig. 4). Therefore, both *B. spathulata* and *B. aculeata* indicate supply of continental
394 degraded organic matter related to riverine discharges during interglacial periods.

395 Interglacial periods were characterized by relatively high P/B ratios (high sea-
396 level) (Figs 4 and 5), as well as warm and humid climate as it is indicated by
397 palynological analyses (Jiménez-Moreno *et al.* 2013). Consequently, a higher humidity
398 might have promoted higher river run-off and more supply of continental degraded
399 organic matter during interglacial periods. This is consistent with the gradual increase of
400 *B. spathulata* concomitant with long-term decrease of 0.7‰ in benthic $\delta^{13}\text{C}$ and 1.4 ‰
401 in planktic $\delta^{13}\text{C}$ as well as low $\delta^{18}\text{O}$ from 5.67 to 5.38 Ma (Fig. 4). Moreover, this
402 agrees with the progressive shallowing upward trend in the core (Pérez-Asensio *et al.*
403 2012b) since continental organic matter reached areas closer to the coast. Very depleted
404 planktic C isotopic values of *Globigerina bulloides* at 5.44 Ma and 5.41 Ma (Figs 4 and
405 5) might also reflect enhanced rainfall as recorded in sediments from the Mallorca shelf
406 during the early Holocene humid phase (Milker *et al.* 2012). Increased humidity could
407 be related to the global warming linked to interglacial stage TG 11 (5.52 Ma) that
408 started before the Miocene-Pliocene boundary and persisted until the mid Pliocene
409 (Vidal *et al.* 2002; Jiménez-Moreno *et al.* 2013). In a global warming context, rainfall
410 would be high (Frei *et al.* 1998) increasing the riverine discharge and providing more
411 degraded terrestrial organic matter to the shelf in the study area.

412 Concerning the oxygen content, the oxygenation is high throughout the studied
413 interval with values higher than 0.8 (Fig. 5). This suggests that oxygen does not control
414 the observed changes in benthic foraminifera. In addition, the presence of an oxygen
415 minimum zone can be ruled out. However, temporary oxygen depletions are recorded
416 along the core (Fig. 5). In the upper slope during glacial periods, they were related with
417 the input of upwelling-related organic matter which reduced the oxygen content due to
418 decay of the organic matter. In the outer shelf during interglacial periods, oxygen

419 decrease was even more severe (Fig. 5) and it was associated with supply of terrestrial
420 organic matter by river run-off.

421

422 *Effect of the MOW interruption on the palaeoproductivity in the northeastern Atlantic*
423 *during the Messinian*

424

425 Low abundance of *U. peregrina* s.l. and high benthic $\delta^{13}\text{C}$ at 6.44 and 6.24 Ma
426 (Fig. 4) indicates a well-ventilated bottom with low organic flux to the sea floor. This
427 indicates the presence of a bottom current, most likely the MOW, because at the
428 present-day as well as during the Quaternary and the Plio-Pleistocene, the MOW has
429 benthic $\delta^{13}\text{C}$ values higher than Atlantic waters reflecting the relatively low residence
430 time of the MOW (Vergnaud-Grazzini 1983; Schönfeld & Zahn 2000; Raddatz *et al.*
431 2011). The MOW would have increased the bottom-water oxygenation as shown by the
432 relatively high oxygen content before the interruption of this current at 6.18 Ma (Figs 5
433 and 6a) when the last open Betic corridor, the Guadalhorce Corridor, was definitively
434 closed (Pérez-Asensio *et al.* 2012a). Furthermore, high benthic $\delta^{13}\text{C}$ could also indicate
435 well-ventilated bottom waters linked to a strong AMOC during interglacial periods as
436 occurs in the Quaternary (Broecker *et al.* 1985).

437 In contrast, high abundance of *U. peregrina* s.l., low benthic $\delta^{13}\text{C}$ at 6.67 and
438 6.35 Ma (Fig. 4) point to the influence of low-oxygen Atlantic upwelled water (AUW)
439 (Fig. 6b). In addition, low benthic $\delta^{13}\text{C}$ could also reflect low ventilation due to a
440 reduced AMOC provoked by low North Atlantic deep water formation during glacial
441 conditions as it has been recorded in the Atlantic and Caribbean Sea during the
442 Messinian (Zahn *et al.* 1997; Bickert *et al.* 2004; van der Laan *et al.* 2012) (Fig. 6b).

443 Hence, the AMOC was weaker during glacial periods than during interglacial periods as
444 occurred in the Quaternary (Broecker *et al.* 1985).

445 After the closure of the Guadalhorce Corridor at 6.18 Ma, there is a gradual
446 decrease of 0.8‰ in the benthic $\delta^{13}\text{C}$ signature that is related with the interruption of the
447 MOW and the influence of oxygen-depleted AUW (Figs 4 and 6c). The planktic $\delta^{13}\text{C}$
448 shows a progressive decrease of 1.3‰ indicating also a higher influence of nutrient-rich
449 AUW. Concomitantly, *U. peregrina* s.l., which thrives under upwelling conditions,
450 gradually increases reaching its highest abundance (Fig. 4). Therefore, after the
451 cessation of the MOW only AUW reached the upper slope in the study area promoting
452 high productivity related to upwelling currents (Fig. 6c). In addition, high productivity
453 could have been favored by the cessation of the MOW, which weakened the AMOC and
454 promoted northern hemisphere cooling, as shown by the onset of small growth of ice
455 sheets in the Iceland-Norwegian Sea and Baffin Bay (Alaska) at ~ 7-6 Ma (Fronval &
456 Jansen 1996; Thiede *et al.* 1998; Pérez-Asensio *et al.* 2012a). This cooling would
457 intensify trade winds that enhance upwelling (Hughen *et al.* 1996; Clark *et al.* 2002).
458 Similarly, a reduced AMOC associated to high productivity has also been recorded in
459 the SE Atlantic Ocean during the Messinian, although in this region intensification of
460 trade winds is related to southern hemisphere cooling (Rommerskirchen *et al.* 2011). On
461 the contrary, as mentioned above sediments from the shelf-edge were particularly
462 oligotrophic. This local low productivity might have been likely produced by a current
463 along the shelf-break that prevented the AUW from reaching the study area between
464 5.87 to 5.77 Ma (Fig. 6d).

465

466 **Conclusions**

467

468 Palaeoproductivity changes and organic carbon cycling in the northeastern
469 Atlantic during the Messinian were controlled by global glacioeustasy. Glacial periods
470 (cold and dry climate) were characterized by high planktic and benthic $\delta^{18}\text{O}$, low
471 benthic $\delta^{13}\text{C}$, low sea-level, high abundance of *U. peregrina* s.l and moderate oxygen
472 depletion. These proxies point to high productivity, related to upwelling currents during
473 glacial periods. These upwelling currents were produced by Ekman pumping due to
474 intensified upwelling-favourable northwesterly trade winds. On the contrary,
475 interglacial periods (warm and humid climate) show low planktic and benthic $\delta^{18}\text{O}$,
476 high sea-level, high oxygen depletion and high abundance of *B. subulata* in the upper
477 slope, and *B. spathulata* and *B. aculeata* in the outer shelf. These indicators suggest
478 presence of more degraded marine organic matter in the upper slope and supply of
479 degraded continental organic matter derived from river run-off in the outer shelf.

480 Before the closure of the Guadalhorce Corridor, the last Betic Atlantic-
481 Mediterranean gateway to be active, the study area was alternatively influenced by well-
482 ventilated MOW and the poorly ventilated AUW. Once this Betic seaway was closed at
483 6.18 Ma, the interruption of the MOW reduced the AMOC and promoted glacial
484 conditions in the northern hemisphere, thus favouring high productivity conditions. This
485 shows how the cessation of the MOW due to the closure of the Guadalhorce Corridor
486 caused global oceanographic and climatic changes affecting productivity in the northern
487 hemisphere. In addition, the variability of the AMOC was recorded by fluctuations in
488 the benthic $\delta^{13}\text{C}$. High benthic $\delta^{13}\text{C}$ indicates well-ventilated bottom waters due to
489 strong AMOC during interglacial periods. In contrast, low benthic $\delta^{13}\text{C}$ reflect poor
490 ventilation as a result of weak AMOC during glacial periods.

491

492 We are very grateful to two anonymous reviewers and the editor Dr. Jim Hendry for
493 their thorough review on an early version of the manuscript. Their comments and
494 suggestions have been very valuable to improve the quality of the paper. This work was
495 funded by the Research Projects CGL2010-20857 and CGL2009-11539/BTE of the
496 Ministerio de Ciencia e Innovación of Spain, and the Research Group RNM-190 of the
497 Junta de Andalucía. JNPA was funded by a research F.P.U. grant (ref. AP2007-00345)
498 awarded by the Ministerio de Educación of Spain. We want to thank N. Andersen
499 (Leibniz-Laboratory, Kiel, Germany) for stable isotope analysis.

500

501 **References:**

502

503 ABRANTES, F. 1991. Variability of upwelling off NW Africa during the latest

504 Quaternary: Diatom evidence. *Paleoceanography*, **6**, 431–460, doi:

505 10.1029/91PA00049.

506 ABRANTES, F. 2000. 200000 yr diatom records from Atlantic upwelling sites reveal

507 maximum productivity during LGM and a shift in phytoplankton community

508 structure at 185000 yr. *Earth and Planetary Science Letters*, **176**, 7–16, doi:

509 10.1016/S0012-821X(99)00312-X.

510 AGUIRRE, J. 1992. Evolución de las asociaciones fósiles del Plioceno marino de Cabo

511 Roche (Cádiz). *Revista Española de Paleontología Extra*, **3**, 3–10.

512 AGUIRRE, J. 1995. Implicaciones paleoambientales y paleogeográficas de dos

513 discontinuidades estratigráficas en los depósitos pliocénicos de Cádiz (SW de

514 España). *Revista de la Sociedad Geológica de España*, **8**, 161–174.

515 AGUIRRE, J., CASTILLO, C., FÉRRIZ, F.J., AGUSTÍ, J. & OMS, O. 1995. Marine-continental

516 magnetobiostratigraphic correlation of the *Dolomys* subzone (middle of Late

517 Ruscinian): Implications for the Late Ruscinian age. *Palaeogeography,*
518 *Palaeoclimatology, Palaeoecology*, **117**, 139–152, doi:10.1016/ 0031-
519 0182(94)00123-P.

520 AGUIRRE, J., BRAGA, J.C. & MARTÍN, J.M. 2007. El Mioceno marino del Prebético
521 occidental (Cordillera Bética, SE de España): Historia del cierre del Estrecho
522 Norbético. *In*: AGUIRRE, J., COMPANY, M. & RODRÍGUEZ-TOVAR, F.J. (eds.) *XIII*
523 *Jornadas de la Sociedad Española de Paleontología: Guía de Excursiones*. Instituto
524 Geológico y Minero de España, Universidad de Granada, Granada, 53–66.

525 BACETA, J.I., & PENDÓN, J.G. 1999. Estratigrafía y arquitectura de facies de la
526 Formación Niebla, Neógeno superior, sector occidental de la Cuenca del
527 Guadalquivir. *Revista de la Sociedad Geológica de España*, **12**, 419–438.

528 BAKUN, A., FIELD, D.B., REDONDO-RODRIGUEZ, A. & WEEKS S.J. 2010. Greenhouse
529 gas, upwelling-favorable winds, and the future of coastal ocean upwelling
530 ecosystems. *Global Change Biology*, **16**, 1213–1228, doi: 10.1111/j.1365-
531 2486.2009.02094.x.

532 BETZLER, C., BRAGA, J.C., MARTÍN, J.M., SÁNCHEZ-ALMAZO, I.M. & LINDHORST, S.
533 2006. Closure of a seaway: Stratigraphic record and facies (Guadix basin, southern
534 Spain). *International Journal of Earth Sciences*, **95**, 903–910, doi:10.1007/s00531-
535 006-0073-y.

536 BICKERT, T., HAUG, G.H. & TIEDEMANN, R. 2004. Late Neogene benthic stable isotope
537 record of Ocean Drilling Program Site 999: Implications for Caribbean
538 paleoceanography, organic carbon burial, and the Messinian Salinity Crisis.
539 *Paleoceanography*, **19**, doi:10.1029/2002PA000799.

540 BIGG, G.R. & WADLEY, M.R. 2001. Millennial-scale variability in the oceans: an ocean
541 modelling view. *Journal of Quaternary Science*, **16**, 309–319, doi:10.1002/jqs.599.

542 BIGG, G.R., JICKELLS, T.D., LISS, P.S. & OSBORN, T.J. 2003. The role of the oceans in
543 climate. *International Journal of Climatology*, **23**, 1127–1159, doi:10.1002/joc.926.

544 BRAGA, J.C., MARTÍN, J.M. & AGUIRRE, J. 2002. Tertiary. Southern Spain. *In*: Gibbons,
545 W. & Moreno, T. (eds.) *The Geology of Spain*, The Geological Society, London,
546 320–327.

547 BRAGA, J.C., MARTÍN, J.M. & QUESADA, C. 2003. Patterns and average rates of late
548 Neogene-Recent uplift of the Betic Cordillera, SE Spain. *Geomorphology*, **50**, 3–26,
549 doi:10.1016/S0169-555X(02)00205-2.

550 BRAGA, J.C., MARTÍN, J.M., AGUIRRE, J., BAIRD, C.D., GRUNNALEITE, I., JENSEN, N.B.,
551 PUGA-BERNABÉU, A., SAELEN, G. & TALBOT, M.R. 2010. Middle-Miocene
552 (Serravallian) temperate carbonates in a seaway connecting the Atlantic Ocean and
553 the Mediterranean Sea (North Betic Strait, S Spain). *Sedimentary Geology*, **225**, 19–
554 33, doi:10.1016/j.sedgeo.2010.01.003.

555 BROECKER, W.S., PETEET, D.M. & RIND, D. 1985. Does the ocean-atmosphere system
556 have more than one stable mode of operation. *Nature*, **315**, 21–26,
557 doi:10.1038/315021a0.

558 CABEÇADAS, G. & BROGUEIRA, M.J. 1997. Sediments in a Portuguese coastal area —
559 pool sizes of mobile and immobile forms of nitrogen and phosphorus. *Marine and*
560 *Freshwater Research*, **48**, 559–563, doi:10.1071/MF96053.

561 CIVIS, J., SIERRA, F.J., GONZÁLEZ-DELGADO, J.A., FLORES, J.A., ANDRÉS, I., DE PORTA,
562 J. & VALLE, M.F. 1987. El Neógeno marino de la provincia de Huelva: Antecedentes
563 y definición de las unidades litoestratigráficas. *In*: CIVIS, J. (ed.) *Paleontología del*
564 *Neógeno de Huelva*. Ediciones Universidad de Salamanca, Salamanca, 9–21.

- 565 CLARK, P.U., PISIAS, N.G., STOCKER, T.F. & WEAVER, A.J. 2002. The role of the
566 thermohaline circulation in abrupt climate change. *Nature*, **415**, 863–869,
567 doi:10.1038/415863a.
- 568 DIESTER-HAASS, L. & SCHRADER, H.-J. 1979. Neogene coastal upwelling history off
569 northwest and southwest Africa. *Marine Geology*, **29**, 39–53, doi:10.1016/0025-
570 3227(79)90101-4.
- 571 DIZ, P. & FRANCÉS, G. 2008. Distribution of live benthic foraminifera in the Ría de
572 Vigo (NW Spain). *Marine Micropaleontology*, **66**, 165–191,
573 doi:10.1016/j.marmicro.2007.09.001.
- 574 DONNICI, S. & SERANDREI-BARBERO, R. 2002. The benthic foraminiferal communities
575 of the northern Adriatic continental shelf. *Marine Micropaleontology*, **44**, 93–123,
576 doi: 10.1016/S0377-8398(01)00043-3.
- 577 DUCHEMIN, G., JORISSEN, F.J., LE LOC'H, F., ANDRIEUX-LOYER, F., HILY, C. &
578 THOUZEAU, G. 2008. Seasonal variability of living benthic foraminifera from the
579 outer continental shelf of the Bay of Biscay. *Journal of Sea Research*, **59**, 297–319,
580 doi:10.1016/j.seares.2008.03.006.
- 581 EBERWEIN, A. & MACKENSEN, A. 2006. Live and dead benthic foraminifera and test
582 $\delta^{13}\text{C}$ record primary productivity off Morocco (NW-Africa). *Deep-Sea Research*
583 *Part I*, **53**, 1379–1405, doi:10.1016/j.dsr.2006.04.001.
- 584 EBERWEIN, A. & MACKENSEN, A. 2008. Last Glacial Maximum paleoproductivity and
585 water masses off NW-Africa: evidence from benthic foraminifera and stable
586 isotopes. *Marine Micropaleontology*, **67**, 87–103,
587 doi:10.1016/j.marmicro.2007.08.008.
- 588 ESTEBAN, M., BRAGA, J.C., MARTÍN, J.M. & SANTISTEBAN, C. 1996. Western
589 Mediterranean reef complexes. In: FRANSEEN, E.K., ESTEBAN, M., WARD, W.C., &

590 ROUCHY, J.M. (eds.) *Models for Carbonate Stratigraphy from Miocene Reef*
591 *Complexes of Mediterranean Regions. Concepts in Sedimentology and*
592 *Paleontology, vol. 5.* Society of Economic Paleontologists and Mineralogists,
593 Tulsa, 55–72.

594 FONTANIER, C., JORISSEN, F.J., CHAILLOU, G., DAVID, C., ANSCHUTZ, P. & LAFON, V.
595 2003. Seasonal and interannual variability of benthic foraminiferal faunas at 550 m
596 depth in the Bay of Biscay. *Deep-Sea Research I*, **50**, 457–494, doi:10.1016/S0967-
597 0637(02)00167-X.

598 FREI, C., SCHÄR, C., LÜTHI, D. & DAVIES, H.C. 1998. Heavy Precipitation Processes in
599 warmer climate. *Geophysical Research Letters*, **25**, 1431-1434, doi:
600 10.1029/98GL51099.

601 FRONVAL, T. & JANSEN, E. 1996. Late Neogene paleoclimates and paleoceanography in
602 the Iceland-Norwegian Sea: Evidence from the Iceland and VØring Plateaus.
603 *Proceedings of the Ocean Drilling Program, Scientific Results*, **151**, 455–468,
604 doi:10.2973/odp.proc.sr.151.134.1996.

605 GONZÁLEZ-DELGADO, J.A., CIVIS, J., DABRIO, C.J., GOY, J.L., LEDESMA, S., PAIS, J.,
606 SIERRO, F.J. & ZAZO, C. 2004. Cuenca del Guadalquivir. *In*: VERA, J.A. (ed.)
607 *Geología de España*. SGE-IGME, Madrid, 543–550.

608 HAMMER, Ø., HARPER, D.A.T. & RYAN, P.D. 2001. PAST: Paleontological Statistics
609 software package for education and data analysis. *Palaeontologia Electronica*, **4**,
610 1–9.

611 HUGHEN, K.A., OVERPECK, J.T., PETERSON, L.C. & TRUMBORE, S. 1996. Rapid climate
612 changes in the tropical Atlantic region during the last deglaciation. *Nature*, **380**, 51–
613 54, doi:10.1038/380051a0.

614 JIMÉNEZ-MORENO, G., PÉREZ-ASENSIO, J.N., LARRASOÑA, J.C., AGUIRRE, J., CIVIS, J.,
615 RIVAS-CARBALLO, M.R., VALLE-HERNÁNDEZ, M.F. & GONZÁLEZ-DELGADO J.A.
616 2013. Vegetation, sea-level and climate changes during the Messinian salinity crisis.
617 *Geological Society of America Bulletin*, **125**, 432–444, doi:10.1130/B30663.1.

618 JORISSEN, F.J., BARMAWIDJAJA, D.M., PUSKARIC, S. & VAN DER ZWAAN G.J. 1992.
619 Vertical distribution of benthic foraminifera in the northern Adriatic Sea: the relation
620 with the organic flux. *Marine Micropaleontology*, **19**, 131–146, doi: 10.1016/0377-
621 8398(92)90025-F.

622 KOHO, K.A., GARCÍA, R., DE STIGTER, H.C., EPPING, E., KONING, E, KOUWENHOVEN,
623 T.J. & VAN DER ZWAAN, G.J. 2008. Sedimentary labile organic carbon and pore water
624 redox control on species distribution of benthic foraminifera: A case study from
625 Lisbon-Setúbal Canyon (southern Portugal). *Progress in Oceanography*, **79**, 55–82,
626 doi:10.1016/j.pocean.2008.07.004.

627 KOUWENHOVEN, T.J., SEIDENKRANTZ, M.-S. & VAN DER ZWAAN, G.J. 1999. Deep-water
628 changes: the near-synchronous disappearance of a group of benthic foraminifera
629 from the Late Miocene Mediterranean. *Palaeogeography, Palaeoclimatology,*
630 *Palaeoecology*, **152**, 259–281, doi:10.1016/S0031-0182(99)00065-6.

631 LARRASOÑA, J.C., GONZÁLEZ-DELGADO, J.A., CIVIS, J., SIERRO, F.J., ALONSO-
632 GAVILÁN, G. & PAIS, J. 2008. Magnetobiostratigraphic dating and environmental
633 magnetism of Late Neogene marine sediments recovered at the Huelva-1 and
634 Montemayor-1 boreholes (lower Guadalquivir basin, Spain). *Geo-Temas*, **10**, 1175–
635 1178.

636 LEBREIRO, S.M., MORENO, J.C., ABRANTES, F.F. & PFLAUMANN, U. 1997. Productivity
637 and paleoceanographic implications on the Tore Seamount (Iberian Margin) during

638 the last 225 kyr: foraminiferal evidence. *Paleoceanography*, **12**, 718–727,
639 doi:10.1029/97PA01748.

640 LEBREIRO, S.M., FRANCÉS, G., ABRANTES, F.F.G., DIZ, P., BARTELS-JONSDOTTIR, H.B.,
641 STROYNOWSKI, Z.N., GIL, I.M., PENA, L.D., RODRIGUES, T., JONES, P.D., NOMBELA,
642 M.A., ALEJO, I., BRIFFA, K.R., HARRIS, I. & GRIMALT, J.O. 2006. Climate change and
643 coastal hydrographic response along the Atlantic Iberian margin (Tagus Prodelta and
644 Muros Ria) during the last two millennia. *The Holocene*, **16**, 1003–1015,
645 doi:10.1177/0959683606h1990rp.

646 LOURENS, L.J., HILGEN, F.J., SHACKLETON, N.J., LASKAR, J. & WILSON, D.S. 2004. The
647 Neogene Period. *In*: GRADSTEIN, F.M., OGG, J.G. & SMITH, A.G. (eds.) *A Geologic*
648 *Time Scale 2004*. Cambridge University Press, Cambridge, 409–440.

649 LOUTIT, T.S., & KEIGWIN, L.D. 1982. Stable isotopic evidence for latest Miocene sea-
650 level fall in the Mediterranean region. *Nature*, **300**, 163–166, doi:10.1038/300163a0.

651 MACKENSEN, A. 2008. On the use of benthic foraminiferal $\delta^{13}\text{C}$ in palaeoceanography:
652 constraints from primary proxy relationships. *In*: AUSTIN, W.E.N. & JAMES, R.H.
653 (eds.) *Biogeochemical Controls on Palaeoceanographic Environmental Proxies*.
654 Geological Society, London, 121–133.

655 MARTÍN, J.M., BRAGA, J.C. & BETZLER, C. 2001. The Messinian Guadalhorce Corridor:
656 The last northern, Atlantic-Mediterranean gateway. *Terra Nova*, **13**, 418–424,
657 doi:10.1046/j.1365-3121.2001.00376.x.

658 MARTÍN, J.M., BRAGA, J.C., AGUIRRE, J. & PUGA-BERNABÉU, A. 2009. History and
659 evolution of the North-Betic Strait (Prebetic Zone, Betic Cordillera): A narrow, early
660 Tortonian, tidal-dominated, Atlantic-Mediterranean marine passage. *Sedimentary*
661 *Geology*, **216**, 80–90, doi:10.1016/j.sedgeo.2009.01.005.

- 662 MARTINEZ, P., BERTRAND, B., SHIMMIELD, G.B., COCHRANE, K., JORISSEN, J., FOSTER,
663 J.M. & DIGNAN, M. 1999. Upwelling intensity and ocean productivity changes off
664 Cape Blanc (Northwest Africa) during the last 70.000 years: geochemical and
665 micropalaeontological evidence. *Marine Geology*, **158**, 57–74, doi: 10.1016/S0025-
666 3227(98)00161-3.
- 667 MARTINS, V., JOUANNEAU, J.-M., WEBER, O. & ROCHA F. 2006. Tracing the late
668 Holocene evolution of the NW Iberian upwelling system. *Marine*
669 *Micropaleontology*, **59**, 35–55, doi:10.1016/j.marmicro.2005.12.002.
- 670 MAYORAL, E. & PENDÓN, J.G. 1987. Icnofacies y sedimentación en zona costera.
671 Plioceno superior (?), litoral de Huelva. *Acta Geológica Hispánica*, **21–22**, 507–513.
- 672 MCKEE, B.A., ALLER, R.C., ALLISON, M.A., BIANCHI, T.S. & KINEKE G.C. 2004.
673 Transport and transformation of dissolved and particulate materials on continental
674 margins influenced by major rivers: benthic boundary layer and seabed processes.
675 *Continental and Shelf Research*, **24**, 899–926, doi: 10.1016/j.csr.2004.02.009.
- 676 MCMANUS, J.F., FRANCOIS, R. GHERARDI, J.M., KEIGWIN, L.D. & BROWN-LEGER, S.
677 2004. Collapse and rapid resumption of Atlantic meridional circulation linked to
678 deglacial climate changes. *Nature*, **428**, 834–837, doi:10.1038/nature02494.
- 679 MENDES, I., GONZALEZ, R., DIAS, J.M.A., LOBO, F. & MARTINS, V. 2004. Factors
680 influencing recent benthic foraminifera distribution on the Guadiana shelf
681 (Southwestern Iberia). *Marine Micropaleontology*, **51**, 171–192,
682 doi:10.1016/j.marmicro.2003.11.001.
- 683 MILKER, Y., SCHMIEDL, G., BETZLER, C., ANDERSEN, N. & THEODOR, M. 2012.
684 Response of Mallorca shelf ecosystems to an early Holocene humid phase. *Marine*
685 *Micropaleontology*, **90–91**, 1–12, doi:10.1016/j.marmicro.2012.04.001.

686 MOJTAHID, M., JORISSEN, F., DURRIEU, J., GALGANI, F., HOWA, H., REDOIS, F. & CAMPS,
687 R. 2006. Benthic foraminifera as bio-indicators of drill cutting disposal in tropical
688 east Atlantic outer shelf environments. *Marine Micropaleontology*, **61**, 58–75,
689 doi:10.1016/j.marmicro.2006.05.004.

690 MURPHY, L.N., KIRK-DAVIDOFF, D.B., MAHOWALD, N. & OTTO-BLIESNER B.L. 2009. A
691 numerical study of the climate response to lowered Mediterranean Sea level during
692 the Messinian Salinity Crisis. *Palaeogeography, Palaeoclimatology, Palaeoecology*,
693 **279**, 41–59, doi:10.1016/j.palaeo.2009.04.016.

694 MURRAY, J.W. 2006. *Ecology and Applications of Benthic Foraminifera*. Cambridge
695 University Press, Cambridge.

696 NAAFS, B.D.A., STEIN, R., HEFTER, J., KHÉLIFI, N., DE SCHEPPER, S. & HAUG G.H. 2010
697 Late Pliocene changes in the North Atlantic Current. *Earth and Planetary Science*
698 *Letters*, **298**, 434–442, doi:10.1016/j.epsl.2010.08.023.

699 NAIDU, P. & NIITSUMA N. 2004. Atypical $\delta^{13}\text{C}$ signature in *Globigerina bulloides* at the
700 ODP Site 723An (Arabian Sea): implications of environmental changes caused by
701 upwelling. *Marine Micropaleontology*, **53**, 1–10,
702 doi:10.1016/j.marmicro.2004.01.005.

703 PÉREZ-ASENSIO, J.N. & AGUIRRE, J. 2010 Benthic foraminiferal assemblages in
704 temperate coral-bearing deposits from the Late Pliocene. *Journal of Foraminiferal*
705 *Research*, **40**, 61–78, doi: 10.2113/gsjfr.40.1.61.

706 PÉREZ-ASENSIO, J.N., AGUIRRE, J., SCHMIEDL, G. & CIVIS J. 2012a. Impact of restriction
707 of the Atlantic-Mediterranean gateway on the Mediterranean Outflow Water and
708 eastern Atlantic circulation during the Messinian. *Paleoceanography*, **27**, PA3222,
709 doi:10.1029/2012PA002309.

710 PÉREZ-ASENSIO, J.N., AGUIRRE, J., SCHMIEDL, G. & CIVIS J. 2012b. Messinian
711 paleoenvironmental evolution in the lower Guadalquivir Basin (SW Spain) based on
712 benthic foraminifera. *Palaeogeography, Palaeoclimatology, Palaeoecology*, **326–**
713 **328**, 135–151, doi:10.1016/j.palaeo.2012.02.014.

714 PHIPPS, M., JORISSEN, F., PUSCEDDU, A., BIANCHELLI, S. & DE STIGTER, H. 2012. Live
715 benthic foraminiferal faunas along a bathymetrical transect (282-4987 m) on the
716 Portuguese margin (NE Atlantic). *Journal of Foraminiferal Research*, **42**, 66–81,
717 doi: 10.2113/gsjfr.42.1.66.

718 PIOTROWSKI, A.M., GOLDSTEIN, S.L., HEMMING, S.R. & FAIRBANKS, R.G. 2005.
719 Temporal relationships of carbon cycling and ocean circulation at glacial boundaries.
720 *Science*, **307**, 1933–1938, doi: 10.1126/science.1104883.

721 POLI, M.S., MEYERS, P.A. & THUNELL, R.C. 2010. The western North Atlantic record of
722 MIS 13 to 10: Changes in primary productivity, organic carbon accumulation and
723 benthic foraminiferal assemblages in sediments from the Blake Outer Ridge (ODP
724 Site 1058). *Palaeogeography, Palaeoclimatology, Palaeoecology*, **295**, 89–101, doi:
725 10.1016/j.palaeo.2010.05.018.

726 PUJOL, C. & VERGNAUD-GRAZZINI, C. 1995. Distribution patterns of live planktic
727 foraminifers as related to regional hydrography and productive systems of the
728 Mediterranean Sea. *Marine Micropaleontology*, **25**, 187–217, doi: 10.1016/0377-
729 8398(95)00002-I.

730 RADDATZ, J., RÜGGERBERG, A., MARGRETH, S., DULLO, W.-C. & IODP EXPEDITION 307
731 SCIENTIFIC PARTY 2011. Paleoenvironmental reconstruction of Challenger Mound
732 initiation in the Porcupine Seabight, NE Atlantic. *Marine Geology*, **282**, 79–90.
733 doi:10.1016/j.margeo.2010.10.019.

734 RAHMSTORF, S. 1998. Influence of Mediterranean Outflow on climate. *Eos Transactions*
735 *AGU*, **79**, 281–282, doi:10.1029/98EO00208.

736 RIAZA, C. & MARTÍNEZ DEL OLMO, W. 1996. Depositional model of the Guadalquivir-
737 Gulf of Cádiz Tertiary basin. *In*: Friend, P. & Dabrio, C.J. (eds.) *Tertiary Basins of*
738 *Spain*, Cambridge University Press, Cambridge, 330–338.

739 RODRIGUES, T., GRIMALT, J.O., ABRANTES, F., FLORES, J.A. & LEBREIRO, S. 2009.
740 Holocene interdependences of changes in sea surface temperature, productivity and
741 fluvial inputs in the Iberian continental shelf (Tagus mud patch). *Geochemistry,*
742 *Geophysics, Geosystems*, **10**, Q07U06, doi:10.1029/2008GC002367.

743 ROGERSON, M., ROHLING, E.J. & WEAVER, P.P.E. 2006. Promotion of meridional
744 overturning by Mediterranean-derived salt during the last deglaciation.
745 *Paleoceanography*, **21**, PA4101, doi:10.1029/2006PA001306.

746 ROGERSON, M., COLMENERO-HIDALGO, E., LEVINE, R.C., ROHLING, E.J., VOELKER,
747 A.H.L., BIGG, G.R., SCHÖNFELD, J., CACHO, I., SIERRO, F.J., LÖWEMARK, L.,
748 REGUERA, M.I., DE ABREU, L. & GARRICK, K. 2010. Enhanced Mediterranean-
749 Atlantic exchange during Atlantic freshening phases, *Geochemistry, Geophysics,*
750 *Geosystems*, **11**, Q08013, doi:10.1029/2009GC002931.

751 ROGERSON, M., ROHLING, E.J., BIGG, G.R. & RAMIREZ, J. 2012. Paleoceanography of
752 the Atlantic-Mediterranean exchange: Overview and first quantitative assessment of
753 climatic forcing. *Reviews of Geophysics*, **50**, RG2003, doi:10.1029/2011RG000376.

754 ROMMERSKIRCHEN, F., CONDON, T., MOLLENHAUER, G., DUPONT, L. & SCHEFUSS E.
755 2011. Miocene to Pliocene development of surface and subsurface temperatures in
756 the Benguela Current system. *Paleoceanography*, **26**, PA3216.
757 doi:10.1029/2010PA002074.

758 SALGUEIRO, E., VOELKER, A.H.L., DE ABREU, L., ABRANTES, F., MEGGERS, H. &
759 WEFER, G. 2010. Temperature and productivity changes off the western Iberian
760 margin during the last 150 ky. *Quaternary Science Reviews*, **29**, 680–695,
761 doi:10.1016/j.quascirev.2009.11.013.

762 SANZ DE GALDEANO, C. & VERA, J.A. 1992. Stratigraphic record and
763 palaeogeographical context of the Neogene basins in the Betic Cordillera, Spain.
764 *Basin Research*, **4**, 21–36, doi:10.1111/j.1365-2117.1992.tb00040.x.

765 SCHMIEDL, G. & MACKENSEN, A. 1997. Late Quaternary paleoproductivity and deep
766 water circulation in the eastern South Atlantic Ocean: Evidence from benthic
767 foraminifera. *Marine Micropaleontology*, **130**, 43–80, doi:10.1016/S0031-
768 0182(96)00137-X.

769 SCHMIEDL, G. & LEUSCHNER, D.C. 2005. Oxygenation changes in the deep western
770 Arabian Sea during the last 190,000 years: productivity versus deepwater circulation.
771 *Paleoceanography*, **20**, PA2008, doi:10.1029/2004PA001044.

772 SCHMIEDL, G., MACKENSEN, A. & MÜLLER, P.J. 1997. Recent benthic foraminifera from
773 the eastern South Atlantic Ocean: Dependence on food supply and water masses.
774 *Marine Micropaleontology*, **32**, 249–287, doi: 10.1016/S0377-8398(97)00023-6.

775 SCHMIEDL, G., DE BOVÉE, F., BUSCAIL, R., CHARRIÈRE, B., HEMLEBEN, C., MEDERNACH,
776 L. & PICON, P. 2000. Trophic control of benthic foraminiferal abundance and
777 microhabitat in the bathyal Gulf of Lions, western Mediterranean Sea. *Marine*
778 *Micropaleontology*, **40**, 167–188, doi: 10.1016/S0377-8398(00)00038-4.

779 SCHMIEDL, G., MITSCHLE, A., BECK, S., EMEIS, K.-C., HEMLEBEN, C., SCHULZ, H.,
780 SPERLING, M. & WELDEAB, S. 2003. Benthic foraminiferal record of ecosystem
781 variability in the Eastern Mediterranean Sea during times of sapropel S5 and S6

782 deposition. *Palaeogeography, Palaeoclimatology, Palaeoecology*, **190**, 139–164,
783 doi:10.1016/S0031-0182(02)00603-X.

784 SCHMIEDL, G., KUHN, T., EHRMANN, W., EMEIS, K.-C., HAMANN, Y., KOTTHOFF, U.,
785 DULSKI, P. & PROSS, J. 2010. Climatic forcing of eastern Mediterranean deep-water
786 and benthic ecosystems during the past 22 000 years, *Quaternary Science Reviews*,
787 **29**, 3006–3020, doi:10.1016/j.quascirev.2010.07.002.

788 SCHÖNFELD, J. & ZAHN, R. 2000. Late Glacial to Holocene history of the Mediterranean
789 Outflow. Evidence from benthic foraminiferal assemblages and stable isotopes at the
790 Portuguese margin. *Palaeogeography Palaeoclimatology Palaeoecology*, **159**, 85–
791 111, doi:10.1016/S0031-0182(00)00035-3.

792 SIERRA, F.J., FLORES, J.A., CIVIS, J., GONZÁLEZ-DELGADO, J.A. & FRANCÉS, G. 1993.
793 Late Miocene globorotaliid event-stratigraphy and biogeography in the NE-Atlantic
794 and Mediterranean. *Marine Micropaleontology*, **21**, 143–167, doi:10.1016/0377-
795 8398(93)90013-N.

796 SIERRA, F.J., GONZÁLEZ-DELGADO, J.A., DABRIO, C.J., FLORES, J.A. & CIVIS, J. 1996.
797 Late Neogene depositional sequences in the foreland basin of Guadalquivir (SW
798 Spain). In: FRIEND, P. & DABRIO, C.J. (eds.) *Tertiary Basins of Spain*. Cambridge
799 University Press, Cambridge, 339–345.

800 THIEDE, J., WINKLER, A., WOLF-WELLING, T., ELDHOLM, O., MYHRE, A.M., BAUMANN,
801 K.-H., HENRICH, R. & STEIN R. 1998. Late Cenozoic history of the polar North
802 Atlantic: Results from ocean drilling. *Quaternary Science Reviews*, **17**, 185–208,
803 doi:10.1016/S0277-3791(97)00076-0.

804 TOMCZAK, M. & GODFREY, J.S. 1994. *Regional oceanography: An introduction*.
805 Pergamon, Oxford.

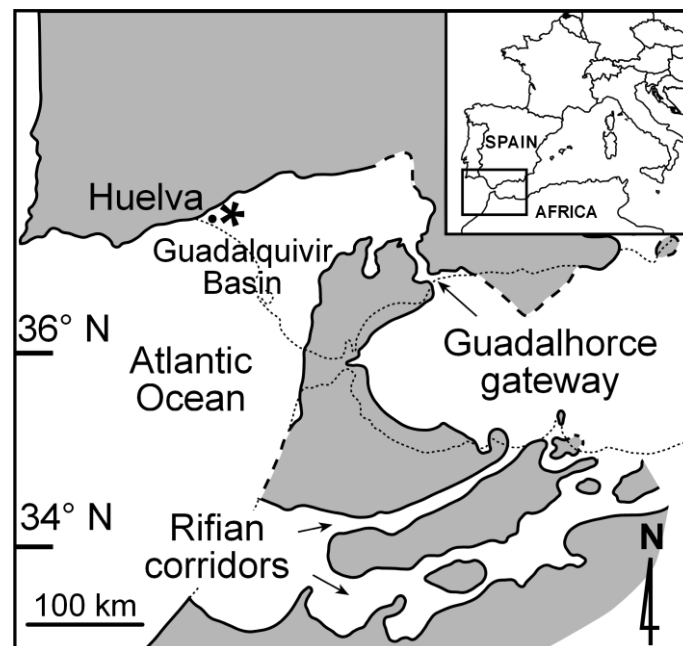
- 806 VAN DER LAAN, E., SNEL, E., DE KAENEL, E., HILGEN, F.J. & KRIJGSMAN, W. 2006. No
807 major deglaciation across the Miocene-Pliocene boundary: integrated stratigraphy
808 and astronomical tuning of the Loulja sections (Bou Regreg area, NW Morocco).
809 *Paleoceanography*, **21**, PA3011, doi:10.1029/2005PA001193.
- 810 VAN DER LAAN, E., HILGEN, F.J., LOURENS, L.J., DE KAENEL, E., GABOARDI, S. &
811 IACCARINO, S. 2012. Astronomical forcing of Northwest African climate and glacial
812 history during the late Messinian (6.5–5.5 Ma). *Palaeogeography*,
813 *Palaeoclimatology, Palaeoecology*, **313–314**, 107–126,
814 doi:10.1016/j.palaeo.2011.10.013.
- 815 VAN DER ZWAAN, G.J. & JORISSEN, F.J. 1991. Biofacial patterns in river-induced shelf
816 anoxia. In: TYSON, R.V. & PEARSON, T.H. (eds.) *Modern and Ancient Continental*
817 *Shelf Anoxia*. Geological Society, Special Publications, 58, London, 65–82.
- 818 VERA, J.A. 2000. El Terciario de la Cordillera Bética: Estado actual de conocimientos.
819 *Revista de la Sociedad Geológica de España*, **13**, 345–373.
- 820 VERGNAUD-GRAZZINI, C. 1983. Reconstruction of Mediterranean Late Cenozoic
821 hydrography by means of carbon isotope analyses. *Utrecht Micropaleontological*
822 *Bulletins*, **30**, 25–47.
- 823 VIDAL, L., BICKERT, T., WEFER, G. & RÖHL, U. 2002. Late Miocene stable isotope
824 stratigraphy of SE Atlantic ODP Site 1085: Relation to Messinian events. *Marine*
825 *Geology*, **180**, 71–85, doi:10.1016/S0025-3227(01)00206-7.
- 826 VILLANUEVA-GUIMERANS, P. & CANUDO, I. 2008. Assemblages of recent benthic
827 foraminifera from the northeastern Gulf of Cádiz. *Geogaceta*, **44**, 139–142.
- 828 VINCENT, E., KILLINGLEY, J.S. & BERGER, W.H. 1980. The magnetic epoch-6 carbon
829 shift: A change in the ocean's $^{13}\text{C}/^{12}\text{C}$ ratio 6.2 million years ago. *Marine*
830 *Micropaleontology*, **5**, 185–203, doi: 10.1016/0377-8398(80)90010-9.

831 WALSH, J.J. 1991. Importance of continental margins in the marine biogeochemical
832 cycling of carbon and nitrogen. *Nature*, **350**, 53–55, doi:10.1038/350053a0.
833 ZAHN, R., SCHÖNFELD, J., KUDRASS, H.R., PARK, M.H., ERLLENKEUSER, H. & GROOTES,
834 P. 1997. Thermohaline instability in the North Atlantic during meltwater events:
835 stable isotope and ice-rafted detritus records from core SO75-26KL, Portuguese
836 margin. *Paleoceanography*, **12**, 696–710, doi: 10.1029/97PA00581.
837 ZARRIESS, M. & MACKENSEN, A. 2010. The tropical rainbelt and productivity changes
838 off northwest Africa: A 31,000-year high-resolution record. *Marine*
839 *Micropaleontology*, **76**, 76–91, doi:10.1016/j.marmicro.2010.06.001.

840

841 **Figures**

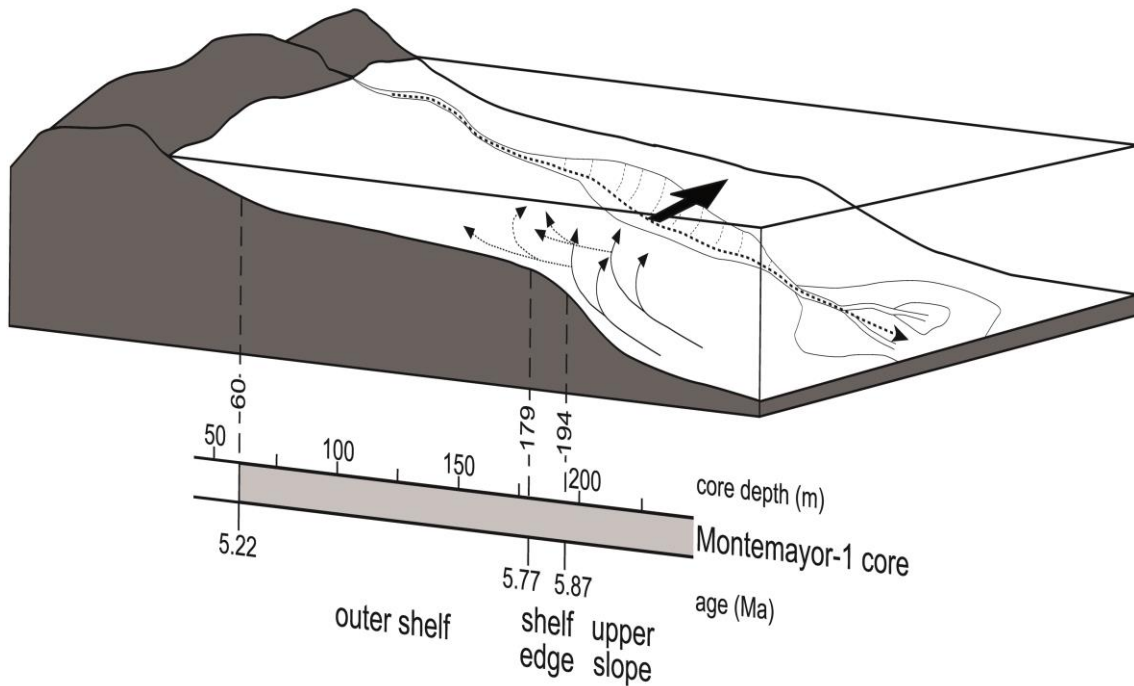
842



843

844 **Fig. 1.** Palaeogeography of the Guadalquivir Basin and the Gibraltar Arc area during the
845 early Messinian (based on Martín et al., 2009). Asterisk points to the location of the
846 Montemayor-1 core.

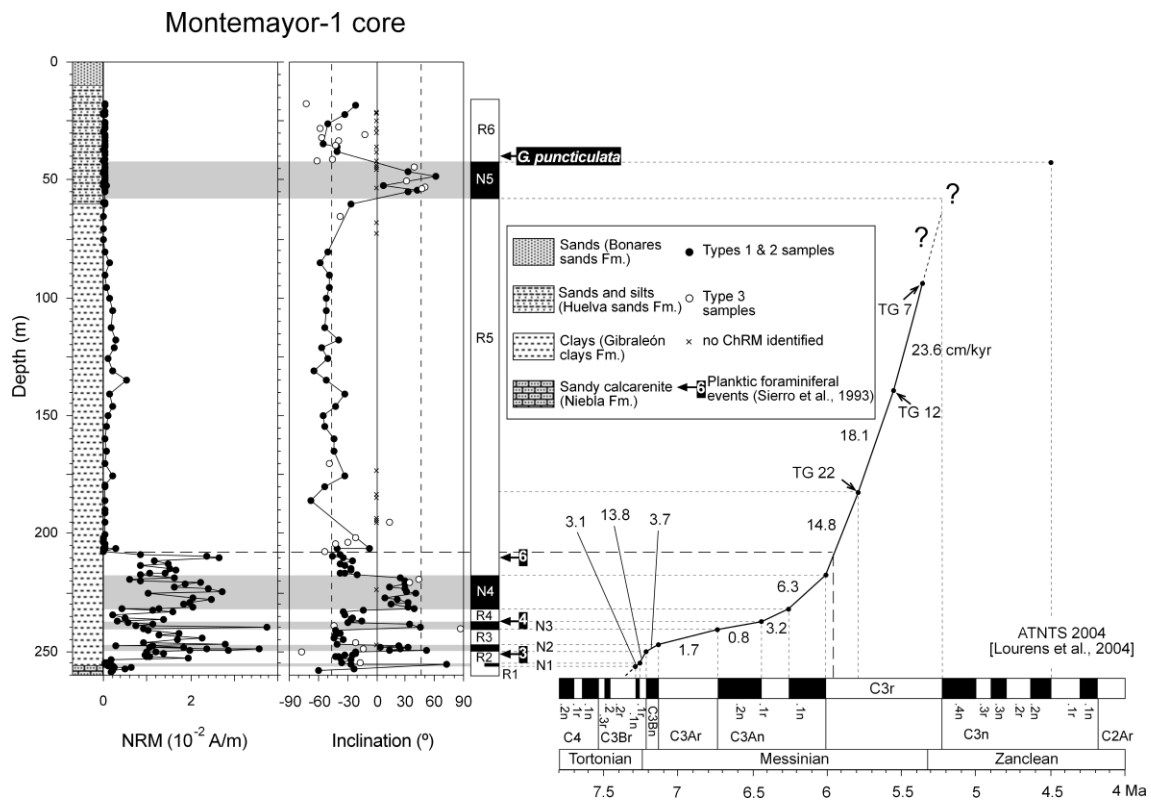
847



848

849 **Fig. 2.** Sketch showing the different palaeoenvironments of the Montemayor-1 core
 850 during the Messinian (upper slope, shelf edge, outer shelf). The main organic matter
 851 sources are shown: thin arrows indicate upwelling currents in the upper slope; thin
 852 dashed arrows denote upwelling currents entering the outer shelf; and thick dashed thick
 853 arrow represents river run-off. Thick arrow shows a superficial current along the shelf
 854 edge (see also Fig. 6d).

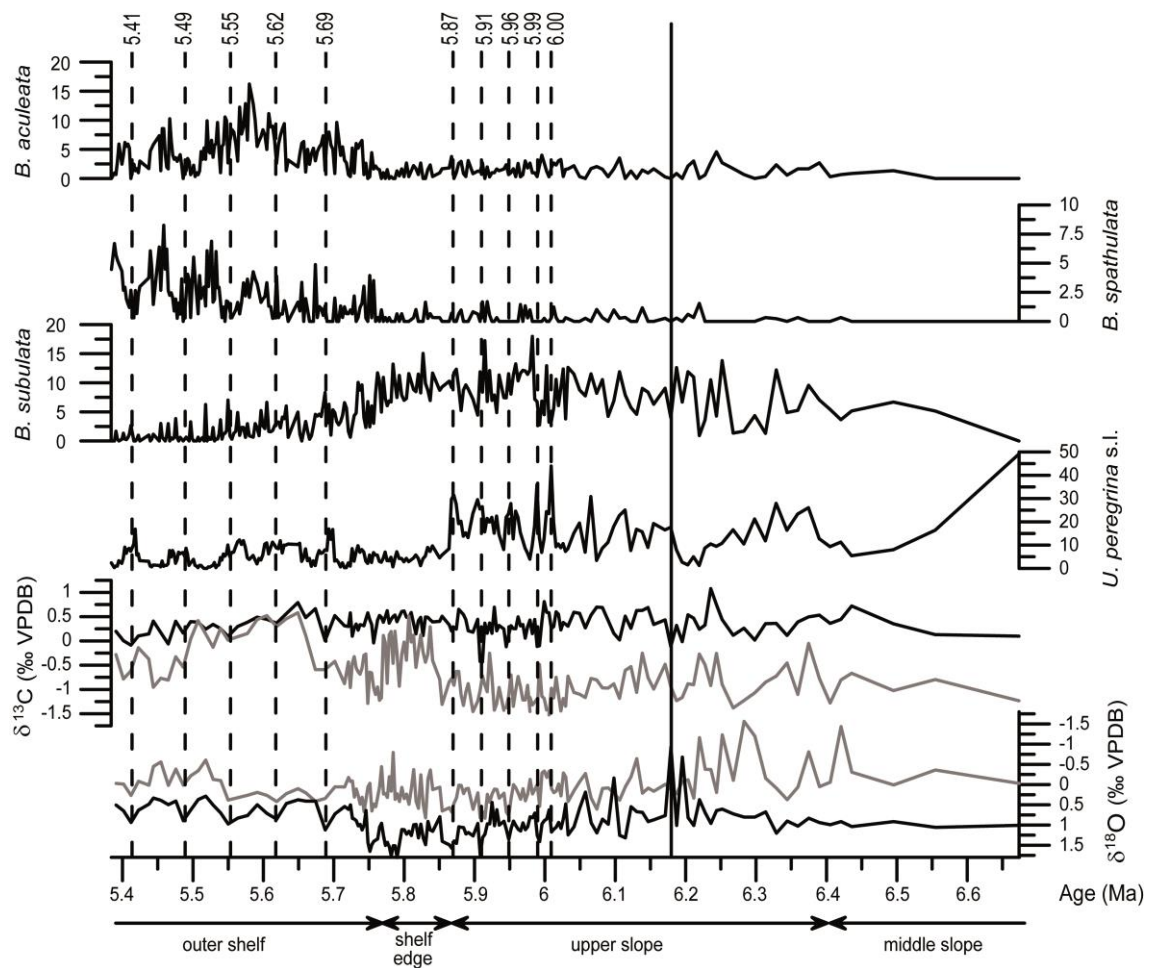
855



856

857 **Fig. 3.** Lithology, age model, sedimentation rate (estimated in cm/kyr) and
 858 magnetobiostratigraphic framework for the Montemayor-1 core (based on Jiménez-
 859 Moreno *et al.* (2013)). Magnetostratigraphy was established according to the
 860 ATNTS2004 (Lourens *et al.* 2004). Type 1 samples have higher quality than types 2 &
 861 3 samples (data from Larrasoña *et al.* (2008)). CrRM stands for characteristic remanent
 862 magnetization. Biostratigraphy is based on the planktonic foraminiferal events (PF
 863 events) of Sierro *et al.* (1993) and first occurrence of *Globorotalia puncticulata*.
 864 Position of glacial stages TG 22 and 12, and interglacial stage 7 are shown. Question
 865 marks indicate uncertainties in the chronology and sedimentation rate.

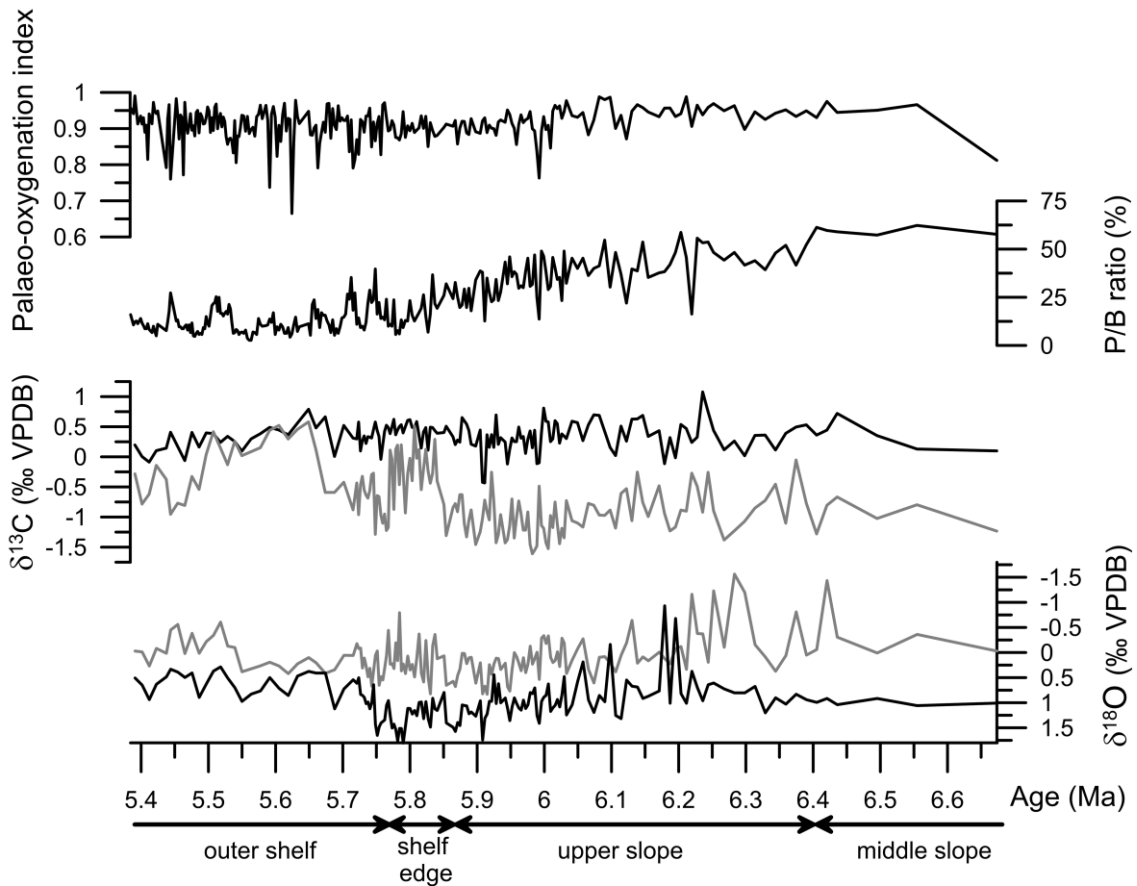
866



867

868 **Fig. 4.** From top to bottom: relative abundances (%) of high-productivity target taxa
 869 including species related to degraded continental organic matter (*Bulimina aculeata*,
 870 *Brizalina spathulata*), degraded marine organic matter (*Bulimina subulata*), and fresh
 871 marine organic matter (*Uvigerina peregrina* s.l.) and; benthic (black) and planktic
 872 (grey) $\delta^{13}\text{C}$ records and benthic (black) and planktic (grey) $\delta^{18}\text{O}$ records in ‰ VPDB of
 873 the Montemayor-1 core. The vertical dashed lines indicate ten events of high
 874 productivity related to upwelling currents in the upper slope (6.00, 5.99, 5.96, 5.91 and
 875 5.87 Ma) and in the outer shelf (5.69, 5.62, 5.55, 5.49, and 5.41 Ma). The vertical black
 876 solid line at 6.18 Ma marks the end of the Atlantic-Mediterranean Betic connection
 877 through the Guadalhorce Corridor. Distribution of palaeoenvironmental settings at the

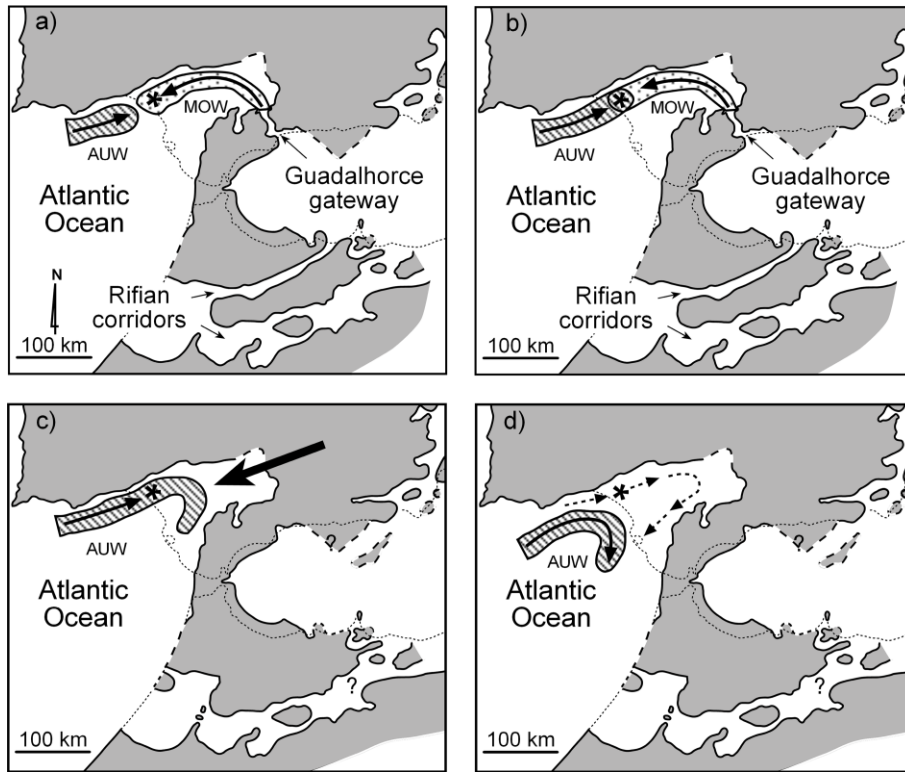
878 bottom of the figure is based on benthic foraminiferal assemblages (Pérez-Asensio *et al.*
879 2012b).
880



881

882 **Fig. 5.** From top to bottom: palaeo-oxygenation index (Schmiedl *et al.* 2003); P/B ratio
883 (%) (Pérez-Asensio *et al.* 2012b) and; benthic (black) and planktic (grey) $\delta^{13}\text{C}$ records
884 and benthic (black) and planktic (grey) $\delta^{18}\text{O}$ records in ‰ VPDB of the Montemayor-1
885 core. Distribution of palaeoenvironmental settings at the bottom of the figure is based
886 on benthic foraminiferal assemblages (Pérez-Asensio *et al.* 2012b).

887



888

889 **Fig. 6.** Palaeogeographical and paleoceanographical evolution of the lower
 890 Guadalquivir Basin during the Messinian (based on Martín *et al.* (2009)). **(a)**
 891 Interglacial conditions before 6.18 Ma, when only the Mediterranean Outflow Water
 892 (MOW) reached the studied core (asterisk). **(b)** Glacial conditions before 6.18 Ma,
 893 when the Atlantic Upwelled Water (AUW) and the MOW reached the studied core. **(c)**
 894 Glacial conditions after 6.18 Ma, when only AUW reached the core because the MOW
 895 was interrupted. The black thick arrow marks the progradation of the main depositional
 896 systems along the axis of the Guadalquivir Basin. **(d)** Studied core (asterisk) influenced
 897 by a current along the shelf-break (dashed arrows) that prevented the AUW from
 898 reaching the study area between 5.87 to 5.77 Ma.